

EVIDENCE FOR MORPHOLOGY AND LUMINOSITY TRANSFORMATION OF GALAXIES AT HIGH REDSHIFTS

HO SEONG HWANG AND CHANGBOM PARK
School of Physics, Korea Institute for Advanced Study, Seoul 130-722, Korea
Last updated: November 8, 2018

ABSTRACT

We study the galaxy morphology-luminosity-environmental relation and its redshift evolution using a spectroscopic sample of galaxies in the Great Observatories Origins Deep Survey (GOODS). In the redshift range of $0.4 \leq z \leq 1.0$ we detect conformity in morphology between neighboring galaxies. The realm of conformity is confined within the virialized region associated with each galaxy plus dark matter halo system. When a galaxy is located within the virial radius of its nearest neighbor galaxy, its morphology strongly depends on the neighbor's distance and morphology: the probability for a galaxy to be an early type (f_E) strongly increases as it approaches an early-type neighbor, but tends to decrease as it approaches a late-type neighbor. We find that f_E evolves much faster in high density regions than in low density regions, and that the morphology-density relation becomes significantly weaker at $z \approx 1$. This may be because the rate of galaxy-galaxy interactions is higher in high density regions, and a series of interactions and mergers over the course of galaxy life eventually transform late types into early types. We find more isolated galaxies are more luminous, which supports luminosity transformation through mergers at these redshifts. Our results are consistent with those from nearby galaxies, and demonstrate that galaxy-galaxy interactions have been strongly affecting the galaxy evolution over a long period of time.

Subject headings: galaxies: evolution – galaxies: formation – galaxies: general – galaxies: high-redshift

1. INTRODUCTION

The role of environment in determining galaxy properties is one of key issues in galaxy formation and evolution. In particular, galaxy morphology is known to depend on environment. It was first noted by Hubble & Humason (1931) who found a large population of ellipticals and lenticulars in galaxy clusters. Later, systematic studies for the connection between galaxy morphology and environment suggested the morphology-radius relation (Oemler 1974) and the morphology-density relation (MDR; Dressler 1980). MDR was detected in the group environment (Postman & Geller 1984), and was also found in galaxy clusters at redshifts up to 1 (Dressler et al. 1997; Treu et al. 2003; Smith et al. 2005; Postman et al. 2005).

Since the Sloan Digital Sky Survey (SDSS; York et al. 2000) and Two Degree Field Galaxy Redshift Survey (2dFGRS; Colless et al. 2001) have produced unprecedentedly large photometric and spectroscopic data of nearby galaxies, the environmental dependence of galaxy properties in local universe has been extensively revisited (e.g., Goto et al. 2003; Balogh et al. 2004a,b; Tanaka et al. 2004; Blanton et al. 2005; Weinmann et al. 2006; Park et al. 2007, 2008; Park & Choi 2009; Park & Hwang 2008). Among them, Park et al. (2007) found that the environmental dependence of various galaxy properties is almost entirely due to their correlation with morphology and luminosity that depend on the local density. If both morphology and luminosity are fixed, galaxy properties such as color, color gradient, concentration, size, velocity dispersion, and star formation rate (SFR), are nearly independent of the local density. This study was extended by Park et al. (2008) who took

into account the effect of the nearest neighbor galaxy. They found that galaxy morphology depends critically on the small-scale environment, which is characterized by the morphology of the nearest neighbor galaxy and the mass density due to the nearest neighbor galaxy, in addition to the luminosity and the large-scale density. They suggested a unified scenario that the morphology and luminosity of a galaxy change through a series of galaxy-galaxy interactions and mergers.

More recently, Park & Choi (2009) investigated the dependence of galaxy properties on both the small- and large-scale environments. They found two characteristic pair-separation scales where the galaxy properties abruptly change: the virial radius $r_{\text{vir,nei}}$ of the nearest neighbor galaxy where the effects of galaxy interaction emerge and $\sim 0.05 r_{\text{vir,nei}}$ where the galaxies in a pair start to merge. The role of large-scale density is weak when morphology and luminosity are fixed. Park & Hwang (2008) reported that the morphology transformation in massive galaxy clusters is driven by hydrodynamic interactions between galaxies and by repeated gravitational interactions among galaxies or between galaxies and their host cluster. Surprisingly, the galaxy morphology does not depend on the local galaxy number density at fixed luminosity and fixed nearest neighbor separation. They found that the morphology-radius relation exists within the cluster virial radius but that galaxy morphology is determined almost entirely by the nearest neighbor distance and morphology outside the cluster virial radius. The MDR is only an apparent phenomenon through the statistical correlation of the local galaxy number density with luminosity and the nearest neighbor distance.

The MDR beyond the local universe, was investigated mostly in high density regions of galaxy clus-

ters (Dressler et al. 1997; Treu et al. 2003; Smith et al. 2005; Postman et al. 2005; see also Poggianti et al. 2008). However, thanks to the recent large, deep-field surveys such as the Great Observatories Origins Deep Survey (GOODS; Giavalisco et al. 2004), the All-Wavelength Extended Groth Strip International Survey (AEGIS; Davis et al. 2007), the VIMOS VLT Deep Survey (VVDS; Le Fèvre et al. 2005), the Cosmic Evolution Survey (COSMOS; Scoville et al. 2007), and the Canada-France-Hawaii Telescope Legacy Survey¹ (CFHTLS), environmental dependence of high redshift ‘field’ galaxy properties has started to be explored: MDR (Nuijten et al. 2005; Capak et al. 2007; van der Wel et al. 2007), color-density relation (CDR) (Cooper et al. 2007; Cucciati et al. 2006; Cassata et al. 2007), and SFR-density relation (Elbaz et al. 2007; Cooper et al. 2008). The MDR and CDR observed locally are also found at high redshifts ($z \sim 1$), but the slope of the relation appears to be different from the local one. It means that galaxy morphology or color evolves differently depending on the background density, in the sense that the stronger evolution is seen in high density regions. Interestingly, the SFR-density relation at high redshifts ($z \sim 1$) is reversed compared to the local one. Namely, the SFR of high redshift galaxies is larger in high density regions than in low density regions (Elbaz et al. 2007; Cooper et al. 2008).

These observational findings raised important questions: (1) whether the correlations between the galaxy properties and the local density are the consequence of environmental-driven evolution; (2) which relation is the most fundamental one (Cooper et al. 2006, 2007; Poggianti et al. 2008). The physical mechanism of environmental effects on the galaxy properties is also poorly understood (Cooper et al. 2006). Moreover, there are few studies that focus on the role of the nearest neighbor galaxy, which turned out to be very important in the evolution of galaxy morphology and luminosity (Park et al. 2008). Since the galaxy interactions and mergers with neighbor galaxies may be more frequent at high redshifts, it is necessary to investigate the role of neighbor galaxies in determining the properties of high redshift galaxies hoping that the main mechanism for galaxy evolution be understood.

In this paper, we study the morphology and luminosity of high redshift galaxies adopting the method similar to that used for nearby SDSS galaxies (Park et al. 2008). Section 2 describes the observational data used in this study. Environmental dependence of galaxy morphology and luminosity is given in §3. Discussion and summary are given in §4 and §5, respectively. Throughout this paper we adopt a flat Λ CDM cosmological model with density parameters $\Omega_\Lambda = 0.73$ and $\Omega_m = 0.27$.

2. DATA

2.1. Observational Data Set

We used a spectroscopic sample of galaxies in GOODS. GOODS is a deep multiwavelength survey covering two carefully selected regions including the Hubble Deep Field North (HDF-N) and the Chandra Deep Field South (CDF-S). Hereafter, two GOODS fields centered

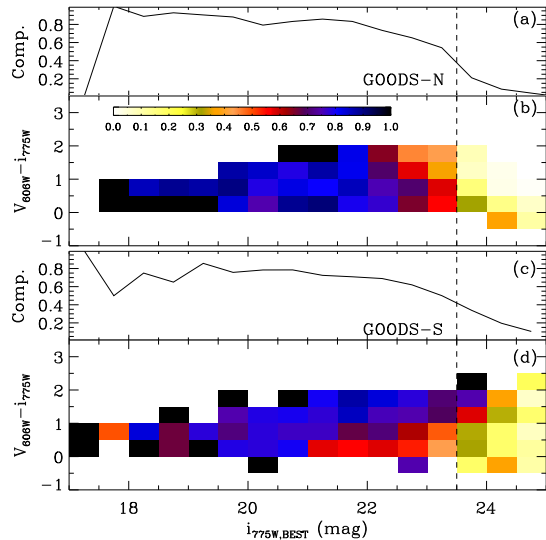


FIG. 1.— Spectroscopic completeness as a function of i -band apparent magnitude (a) and observed color and apparent magnitude (b) of galaxies in GOODS-North. Those for GOODS-South are in (c) and (d). Vertical dashed lines indicate the apparent magnitude limits used in this study.

on HDF-N and CDF-S are called GOODS-North and GOODS-South, respectively. Total observing area is approximately 300 arcmin^2 and each region was observed by NASA’s Great Observatories (*HST*, *Spitzer* and *Chandra*), ESA’s *XMM-Newton*, and several ground-based facilities. *HST* observations with Advanced Camera for Surveys (ACS) were conducted in four bands: B (F435W, 7200s), V (F606W, 5000s), i (F775W, 5000s), and z (F850LP, 10,660s). The drizzled images have a pixel scale of $0.03'' \text{ pixel}^{-1}$ and point-spread function FWHM of $\sim 0.1''$. Spectroscopic data for GOODS sources are enormous in the literature: GOODS-North (Cohen et al. 2000; Cowie et al. 2004; Wirth et al. 2004; Reddy et al. 2006) and GOODS-South (Szokoly et al. 2004; Le Fèvre et al. 2004; Mignoli et al. 2005; Vanzella et al. 2005, 2006, 2008; Ravikumar et al. 2007; Popesso et al. 2009). Among the sources in the ACS photometric catalog, we used 4443 galaxies whose reliable redshifts are available in the literature for further analysis.

Since we are going to investigate the effects of the nearest neighbor galaxies, it is important to identify genuine neighbor galaxies. In addition, since we use a spectroscopic catalog of galaxies combined from various redshift surveys with diverse selection criteria, our sample is heterogeneous. Therefore, it is necessary to know the completeness of our spectroscopic sample accurately. To compute the spectroscopic completeness, we used a sample from the ACS photometric catalog with the objects having SExtractor stellarity class greater than 0.79. The value was chosen from the stellarity distribution of genuine stars confirmed by the spectroscopic observation. In Figure 1, we plot the completeness of each survey as a function of the observed magnitude (SExtractor ‘BEST’ magnitude) and color. It is seen that the completeness decreases significantly near $i_{775W,BEST} \sim 23.5$. The mean completeness at $i_{775W,BEST} \leq 23.5$ is 69% and 63% for GOODS-North and -South, respectively. It is

¹ <http://www.cfht.hawaii.edu/Science/CFHLS/>

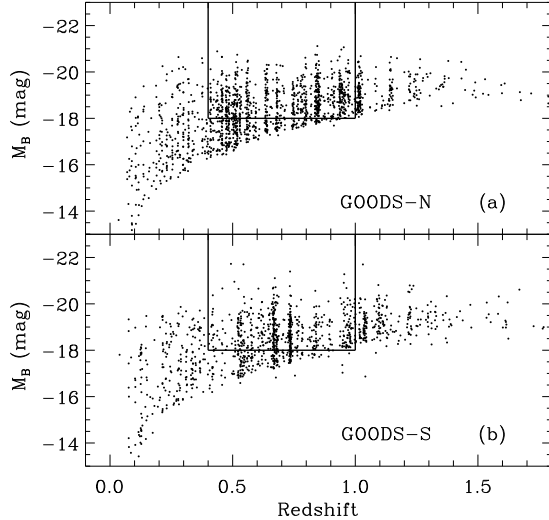


FIG. 2.— Evolution corrected, rest frame M_B vs. redshift for the spectroscopic sample of galaxies in GOODS-North (a) and GOODS-South (b). Solid lines define the volume-limited sample used in this study.

noted that the completeness below the magnitude limit changes significantly with color, which can cause a bias in the studies of galaxy morphology.

The rest frame B -band absolute magnitude M_B of galaxies is computed based on the ACS photometry with Galactic reddening corrections (Schlegel et al. 1998) and K -corrections (Blanton & Roweis 2007). The evolution correction (an increase of $1.3M_B$ per unit redshift) was applied to compute the final rest frame M_B (Faber et al. 2007). In Figure 2, we show the evolution corrected, rest frame M_B as a function of redshift for the sample of galaxies with $i_{775W,BEST} \leq 23.5$. We finally define a volume-limited sample of 1332 galaxies with $M_B \leq -18.0$ and $0.4 \leq z \leq 1.0$ for further analysis.

2.2. Morphology Classification

For the volume-limited sample of galaxies shown in Figure 2, we visually inspected the images in individual ($Bviz$) bands and Bvi pseudo-color images. We divided the galaxies into two morphological types: early types (E/S0) and late types (S/Irr). Early-type galaxies are those with little fluctuation in the surface brightness and color and with good symmetry, while late-type galaxies show internal structures and/or color variations in the pseudo-color images. However, the total color itself is not used as a classification criterion. We checked our results by comparing with the morphological classification of Bundy et al. (2005) who used the same ACS images as ours, and found that 98% of our classifications agree with those of Bundy et al. Some galaxies that were classified as early types in Bundy et al. (2005) are found to be late types in this study because of color variations in the pseudo-color images.

To see how often we classify galaxies differently because we classified galaxies in different wavelength bands across redshift, we made the following experiment. We classified galaxies at $0.4 < z < 0.6$ brighter than $M_B = -18.0$ using their v - or i -band images separately, and checked if the morphological types of each galaxy agree with each other. At $z = 0.9$ the i -band is centered at $\sim 4000\text{\AA}$ in the

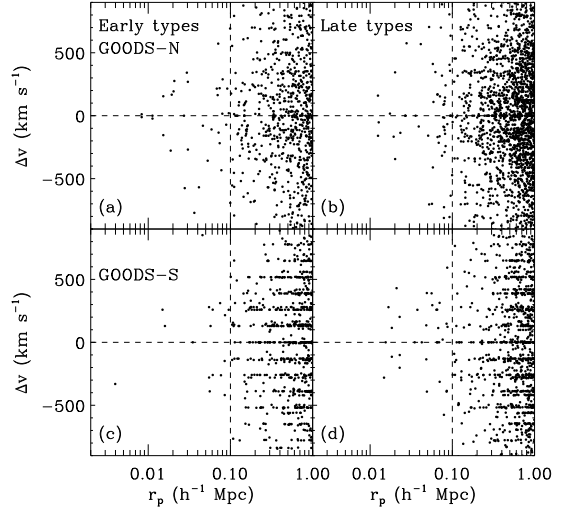


FIG. 3.— Velocity difference between the target galaxies with $-18.5 \geq M_B > -20.0$ and their neighbors brighter than $M_B + 0.5$ as a function of the projected separation. Early- and late-type target galaxies are in left and right panels, respectively. Galaxies of GOODS-North are in (a) and (b), and those of GOODS-South in (c) and (d).

rest frame, and this wavelength roughly corresponds to the v -band at $z \approx 0.5$. We found no galaxy was assigned different morphology. Therefore, our morphology classification is not expected to be affected by the redshift effects.

2.3. Galaxy Environment

We consider two kinds of environmental factors: a surface galaxy number density estimated from five nearest neighbor galaxies (Σ_5) as a large-scale environmental parameter, and the distance to the nearest neighbor galaxy (r_p) as a small-scale environmental parameter.

The background density, Σ_5 , is defined by $\Sigma_5 = 5(\pi D_{p,5}^2)^{-1}$. $D_{p,5}$ is the projected proper distance to the 5th-nearest neighbor. The 5th-nearest neighbor of each target galaxy was identified among the neighbor galaxies with $M_B \leq -18.0$ that have velocities relative to the target galaxy less than 1000 km s^{-1} to exclude foreground and background galaxies.

To define the small-scale environmental parameter attributed to the nearest neighbor, we first find the nearest neighbor of a target galaxy that is closest to the target galaxy on the projected sky and satisfies the conditions of magnitude and relative velocity. We searched for the nearest neighbor galaxy among galaxies that have magnitudes brighter than $M_B = M_{B,\text{target}} + 0.5$ and have relative velocities less than $\Delta v = |v_{\text{neighbors}} - v_{\text{target}}| = 600 \text{ km s}^{-1}$ for early-type target galaxy and less than $\Delta v = 400 \text{ km s}^{-1}$ for late-type target galaxy. These values are the same as those used for selecting the nearest neighbor galaxy in the SDSS data (Park et al. 2008). Since we use the volume-limited sample of galaxies with $M_B \leq -18.0$, we study only the target galaxies brighter than $M_{B,\text{target}} = -18.5$ so that their neighbors are complete.

In Figure 3, we plot the velocity difference for all neighbor galaxies with velocity difference less than 900 km s^{-1} . To fit the velocity distribution, we used the Gaus-

sian plus constant model for each type of target galaxies by combining the data in two surveys. We obtained, for the galaxies at projected proper distance $r_p < 100 h^{-1}$ kpc, the best-fits values $\sigma_{\Delta v} = 351 \pm 48$ and 216 ± 103 km s^{-1} for early- and late-type target galaxies, respectively. It indicates that the velocity limit used for selecting the nearest neighbor is large enough not to miss the neighbor galaxies.

The spectroscopic completeness can affect the identification of the genuine nearest neighbor. The completeness that depends on the apparent magnitude and color as shown in Figure 1, can also depend on the distance between galaxies due to the difficulty in observing galaxies close to each other using multi-object spectrograph (MOS). We checked the completeness as a function of the projected distance to the target galaxy, and found that it does not change with the projected distance. It might be because we combined spectroscopic data from numerous references, therefore, the difficulty in observing nearby galaxies using MOS is significantly reduced.

The virial radius of a galaxy is defined as the radius within which the mean mass density is 200 times the critical density of the universe (ρ_c), and is given by

$$r_{\text{vir}} = (3\gamma L/4\pi/200\rho_c)^{1/3}, \quad (1)$$

where L is the galaxy luminosity, and γ is the mass-to-light ratio. We assume that the mass-to-light ratio of early-type galaxies is on average twice as large as that of late-type galaxies at the same absolute magnitude M_B , which means $\gamma(\text{early}) = 2\gamma(\text{late})$ [see §2.5 of Park & Choi (2009) and §2 of Park et al. (2008)]. The critical density of the universe ρ_c is a function of redshift z and $\Omega_m(z) = \rho_c(z)/\rho_b(z) = \rho_c(z)/\bar{\rho}(1+z)^3$, where ρ_b and $\bar{\rho}$ are the mean matter densities in proper and comoving spaces, respectively. Then, the virial radius of a galaxy at redshift z in proper space can be rewritten by

$$r_{\text{vir}}(z) = [3\gamma L\Omega_{m,0}/800\pi\bar{\rho}/\{\Omega_{m,0}(1+z)^3 + \Omega_{\Lambda,0}\}]^{1/3}. \quad (2)$$

$\Omega_{m,0}$ and $\Omega_{\Lambda,0}$ are the density parameters at the present epoch. We compute the mean mass density $\bar{\rho}$ using the galaxies at $z = 0.4 - 0.7$ with various absolute magnitude limits varying from $M_B = -17.5$ to -20.0 . We found that the mean mass density appears to converge when the magnitude cut is fainter than $M_B = -18.0$, which means that the contribution of faint galaxies is not significant because of their small masses. In this calculation, we weigh each galaxy by an inverse of completeness according to its apparent magnitude and color (see Fig. 1). We obtain $\bar{\rho} = 0.0145(\gamma L)_{-20} (h^{-1}\text{Mpc})^{-3}$ where $(\gamma L)_{-20}$ is the mass of a late-type galaxy with $M_B = -20$. This final value we adopted is computed using all galaxies with $i_{775W,BEST} \leq 23.5$ and $0.4 \leq z \leq 0.7$ to account for the contribution of faint galaxies as much as possible.

If we adopt $\Omega_{m,0} = 0.27$ and $\Omega_{\Lambda,0} = 0.73$, the virial radii of galaxies with $M_B = -18.5$ and -20.0 at $z = 0$ are 220 and 350 h^{-1} kpc for early types, and 180 and 280 h^{-1} kpc for late types, respectively. The proper-space virial radii of galaxies with the same luminosities as above, but located at $z = 1$, are 160 and 250 h^{-1} kpc for early types, and 120 and 200 h^{-1} kpc for late types, respectively.

3. RESULTS

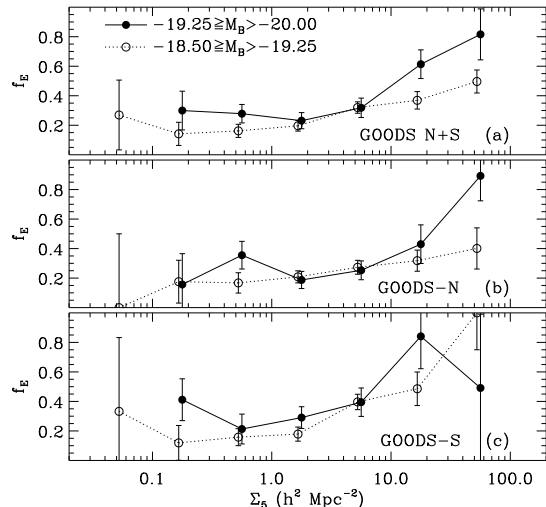


FIG. 4.— Fraction of early-type galaxies in fixed absolute magnitude ranges as a function of Σ_5 . Shown are (a) GOODS-North plus South, (b) GOODS-North, and (c) GOODS-South samples.

3.1. Background Density Dependence of Galaxy Morphology

In Figure 4, we plot the fraction of early-type galaxies as a function of the background density, Σ_5 . To account for the incompleteness shown in Figure 1, the early-type fraction is computed by weighing each galaxy by the inverse of completeness corresponding to its apparent magnitude and color. Each of the volume-limited samples is divided into brighter ($-19.25 \geq M_B > -20.00$) and fainter ($-18.50 \geq M_B > -19.25$) subsamples. The solid and dotted lines are early type-fractions (f_E) for brighter and fainter subsamples, respectively. The uncertainties of the fraction represent 68% (1σ) confidence intervals that are determined by the bootstrap resampling method. Figure 4 clearly shows that the early-type fraction increases along with Σ_5 (i.e., MDR), which is already known in similar high redshift surveys (e.g., Capak et al. 2007). We note that the overall early-type fraction is higher for the brighter subsamples in all surveys. It implies that the morphology-luminosity relation is already well-established at the redshifts under study. The background density dependence of morphology seems stronger for the brighter galaxies. In particular, the early-type fraction of the brighter sample rises sharply at high densities of $\Sigma_5 \gtrsim 10 h^2 \text{Mpc}^{-2}$.

3.2. Effects of the Nearest Neighbor

To measure the effects of the nearest neighbor galaxy on the galaxy morphology, we plot, in Figure 5, the fraction of early-type galaxies as a function of the distance to the nearest neighbor. We can see the probability that a galaxy is found to be an early type, strongly depends on the projected distance to the nearest neighbor galaxy (r_p) as well as neighbor's morphology. When a galaxy is located farther than the virial radius from its nearest neighbor galaxy ($r_p \gtrsim r_{\text{vir,nei}}$), the early-type fraction slowly increases as the distance to the neighbor decreases, but its dependence on neighbor's morphology is weak.

On the other hand, when $r_p \lesssim r_{\text{vir,nei}}$, the early-type fraction increases as the target galaxy approaches an early-type neighbor, but decreases as it approaches a

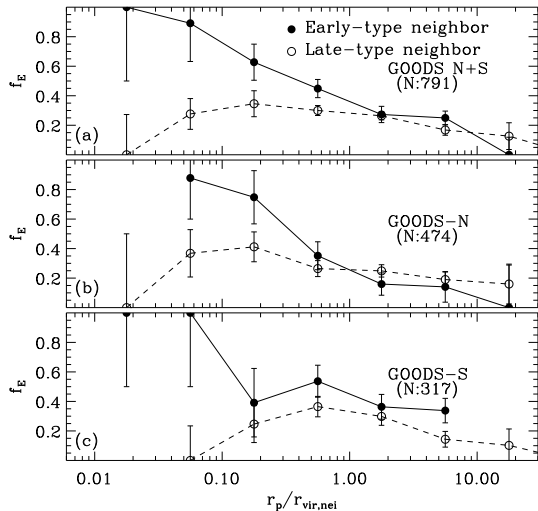


FIG. 5.— Early-type fraction as a function of the distance to the nearest neighbor galaxy. The distance is normalized with respect to the virial radius of the nearest neighbor. Galaxies in the combined GOODS-North plus South sample are used in (a), those of GOODS-North sample in (b), and those of GOODS-South in (c).

late-type neighbor. It is important to note that the bifurcation of the early-type fraction, occurs at $r_p \sim r_{\text{vir,nei}}$. In the case of the cosmology we adopt the radius $r_p = r_{\text{vir,nei}}$ corresponds to the local mass density due to the neighbor of $\rho_n = 740\bar{\rho}$. The bifurcation of the early-type fraction at $r_p \sim r_{\text{vir,nei}}$ is similarly found by Park et al. (2008) using nearby ($z < 0.1$) SDSS galaxies.

To investigate the effects of large-scale environment on the morphology in company with the effects of the nearest neighbor galaxy, we study the early-type fraction in the two-dimensional environmental parameter space as shown in Figure 6. In this case the combined sample of GOODS-North plus South is used. Galaxies are distributed along the diagonal in this figure due to the statistical correlation between r_p and Σ_5 . But there is a significant dispersion in r_p at fixed Σ_5 . It is noted that galaxies are located in wide ranges of Σ_5 and r_p for both early- and late-type neighbor cases even though the early types tend to have relatively larger Σ_5 and smaller r_p . In this figure one can study the dependence of f_E on r_p at each fixed value of Σ_5 by moving along a vertical line.

Figure 6 clearly shows that, when $r_p \lesssim r_{\text{vir,nei}}$, the dependence of morphology on the background density and the nearest neighbor distance becomes completely different when the neighbor’s morphology changes. When the neighbor is a late type, f_E of target galaxies is about 0.2 and is almost independent of r_p or Σ_5 . But when the neighbor is an early type, f_E can rise up to 0.7 when the target galaxy enters a region with the background density exceeding $\Sigma_5 \gg 10h^2\text{Mpc}^{-2}$. There is also a discontinuous rise in f_E when the galaxy approaches the neighbor closer than about $0.3r_{\text{vir,nei}}$, which corresponds to $50 \sim 100h^{-1}\text{kpc}$. When $r_p \gg r_{\text{vir,nei}}$, galaxy morphology is independent of all environmental factors and f_E is about 0.2. It should be emphasized that the difference between the left and right panels of Figure 6 is manifest only when r_p is less than about $2r_{\text{vir,nei}}$. As noted above, a direct effect of the existence of the neighbor on f_E is evident at the neighbor distance of $r_p \lesssim 0.3r_{\text{vir,nei}}$

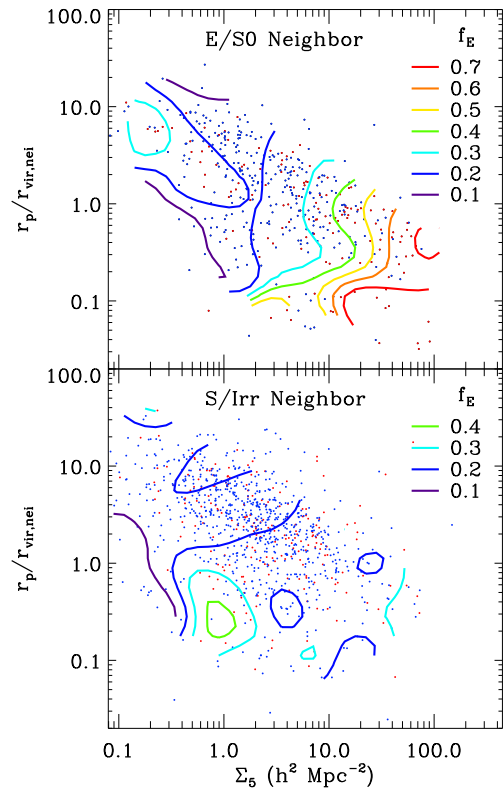


FIG. 6.— Morphology-environment relation when the nearest neighbor galaxy is an early type (upper) or a late type (lower). Contours show constant early-type galaxy fraction f_E . Galaxies used here are brighter than $M_B = -18.5$.

in the case of early-type nearest neighbor. This confirms the net effects of the nearest neighbor on morphology at fixed large-scale environment for the GOODS galaxies. However, the effects of late-type neighbors do not appear as strong as what is seen for the nearby SDSS galaxies (Park & Choi 2009). More data with a higher completeness are needed to confirm it.

In Figure 7, we plot the evolution-corrected, rest frame M_B as a function of the distance to the nearest neighbor for the combined sample of GOODS-North plus South with $M_B \leq -18.5$. The lines show the median value in each projected separation bin. Top panels show that the early-type galaxies having $r_p > r_{\text{vir,nei}}$ are significantly brighter than those at $r_p < r_{\text{vir,nei}}$, while the magnitude difference for late-type galaxies in the two regions is smaller. If we divide the galaxies into those in relatively higher density region ($\Sigma_5 > 6h^2\text{Mpc}^{-2}$) and those in lower density region ($\Sigma_5 \leq 6h^2\text{Mpc}^{-2}$), the increase of galaxy luminosity with increasing r_p is manifest in the high density region.

4. DISCUSSION

4.1. Morphology and Luminosity Transformation

We found in Figure 5 that the morphological types of high redshift galaxies depend critically on the small-scale environment, which is characterized by the morphology of the nearest neighbor galaxy and the distance to the nearest neighbor galaxy. If our results are affected by the trend that the early-type fraction (f_E) is higher when the local density is higher (i.e., MDR), f_E should be a

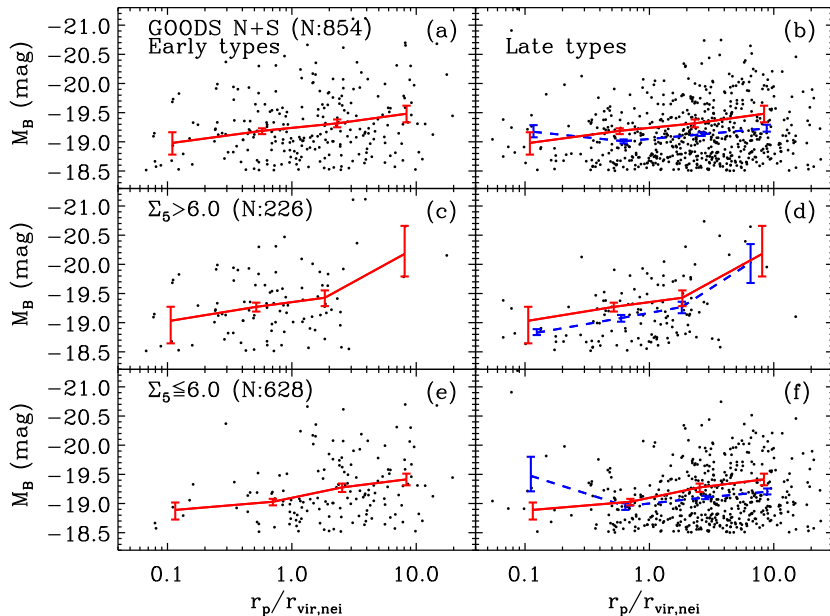


FIG. 7.— Absolute magnitude of early-(left) and late-type (right) galaxies with $M_B \leq -18.5$ and $0.4 \leq z \leq 1.0$ in the GOODS-North plus South sample as a function of the distance to the nearest neighbor galaxy. The median magnitudes of early and late types are represented by solid and dashed curves, respectively. The curves in the left panels are repeated in the right panels as solid curves. Galaxies in all environments are used in (a) and (b), those in high density regions are in (c) and (d), and those in relatively low density regions are in (e) and (f). Number in parenthesis is the number of galaxies in the combined sample or local density subsample.

function of r_p which is independent of the neighbor morphology, and the two curves in the top panel of Figure 5 have the same amplitude at each neighbor separation. The fact that f_E is independent of neighbor morphology at $r_p > r_{\text{vir,nei}}$ but starts to show a significant dependence at $r_p < r_{\text{vir,nei}}$, demonstrates that the neighbor effects are the dominating factor of the change in f_E and the large-scale background density is not.

Increase of f_E with decreasing the neighbor distance at $r_p \gtrsim r_{\text{vir,nei}}$, can be explained by the tidal effects of neighbor galaxy. Park et al. (2008) showed that tidal energy deposit relative to the binding energy for the dark halos of equal mass galaxies, is not negligible at the separation of virial radius. The tidal effects can accelerate the consumption of cold gas, changing late types to early types. In fact, Park & Choi (2009) showed that the center of late-type galaxies becomes bluer by the existence of neighbor galaxies even when $r_p > r_{\text{vir,nei}}$ independently of the morphological type of the neighbor. Their surface brightness and central velocity dispersion increase as the neighbor distance decreases, implying the growth of the bulge component.

The bifurcation of f_E at $r_p \sim r_{\text{vir,nei}}$ was interpreted as due to the hydrodynamic effects of the nearest neighbor (Park et al. 2008). If a target galaxy approaches a late-type neighbor within one virial radius of the neighbor, the cold gas of the neighbor can flow into the target galaxy and the target galaxy tends to become a late type. On the other hand, if the target galaxy approaches an early-type neighbor within one virial radius of the neighbor, the hot gas and the tidal force of the neighbor accelerate the consumption of cold gas so that the target galaxy tends to evolve to an early type.

Moreover, it is noted in Figure 6, that the galaxies tend to be early types when they have close early-type neighbors even though they are in low density regions, and the

galaxies are likely to be late types when they have close late-type neighbors even though they are in high density regions. The galaxy morphology appears to depend on the large-scale background density. But it may be the result of the cumulative effects of neighbor interaction that is stronger in high density regions (Park et al. 2008).

We also found in Figure 7 that isolated galaxies are brighter than less isolated ones. These results can provide important hints for the evolution of galaxies. Previously, Park et al. (2008) obtained results similar to ours using the SDSS data (see their Fig. 6), and suggested a unified scenario as follows. Once the separation of two galaxies becomes small enough, namely $r_p \lesssim 0.05r_{\text{vir,nei}}$ (Park & Choi 2009), they undergo a merger and the merger product will be more massive. The merger product will typically find itself isolated from its neighbors of comparable mass. As galaxies experience a series of merger events, the cold gas will be exhausted due to the merger-induced star formation. Thus the massive galaxies are likely to be early types. As a supporting evidence for this scenario, they showed that, at fixed background density, post-merger features such as large displacement of the galaxy nucleus from the center, turmoil features, and/or very close double cores, are more frequently seen in the isolated galaxies compared to the less isolated ones.

We extended our analysis to another multiwavelength survey, AEGIS, of which survey area (~ 710 arcmin²) is larger than GOODS (~ 300 arcmin²). Using AEGIS data, we measured the early-type fraction of target galaxies as a function of the nearest neighbor distance (e.g., Fig. 5), and found that the early-type fraction does not change significantly with the neighbor distance even though it showed dependence on the large-scale background density. Furthermore, it does not show the bifurcation in accordance with neighbor's morphology. These results are inconsistent with those from GOODS and SDSS samples

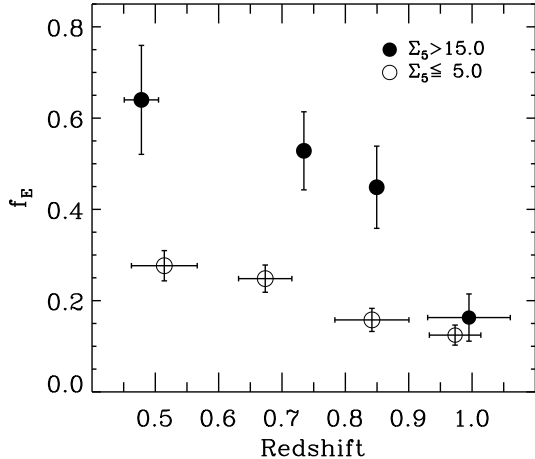


FIG. 8.— Early-type fraction in the combined GOODS-North plus South sample as a function of redshift. Filled and open circles indicate the early-type fraction in high and low density regions, respectively, located at the median redshift in each redshift bin.

(e.g., Park et al. 2008; Park & Choi 2009). The results from AEGIS may have been significantly affected by the low completeness of DEEP2 survey. Since the completeness of DEEP2 spectroscopic survey is only about 0.5, it is expected that the nearest neighbor is seriously misidentified compared to the case using the GOODS or SDSS data. Our Monte Carlo experiment shows that the fraction of the misidentified nearest neighbor reaches about 50% when the sample completeness is 50%. We therefore conclude that it is not appropriate to study galaxy interactions using the DEEP2/AEGIS data.

4.2. Redshift Evolution of Galaxy Morphology

If galaxies transform their morphology through a series of interactions and mergers, it is expected that the high-redshift galaxies, on average, are less massive and richer in cold gas. Successive consumption of cold gas in galaxies through interaction and merger events is likely to transform late types into early types. And then the early-type fraction at high redshifts is expected to be lower compared to that at low redshifts, and the fraction of blue early types among early types to be higher at higher redshifts (Park et al. 2008; Capak et al. 2007; see also Conselice et al. 2005, 2008; Lotz et al. 2008; Menanteau et al. 2004; Lee et al. 2006; Puzia et al. 2007). Moreover, the early-type fraction is expected to evolve differently depending on the background density (Park et al. 2008). Since the mean separation between galaxies is relatively smaller and the merger/interaction rate is higher in high density regions, galaxies are expected to show a stronger time evolution in morphology as well as luminosity, color, and SFR in high density regions. On the contrary, in low density regions where the mean separation between galaxies is larger, the time evolution of galaxies is expected to be slower because the interactions and mergers among galaxies are less frequent.

There have been several studies of the evolution of morphology of high redshift galaxies focusing on the role of environment. For example, Nuijten et al. (2005) used Sérsic index n and the $u^* - g'$ color of galaxies as proxies for galaxy morphology to study galaxy evolution. They found that the number fraction of “bulge-dominated”

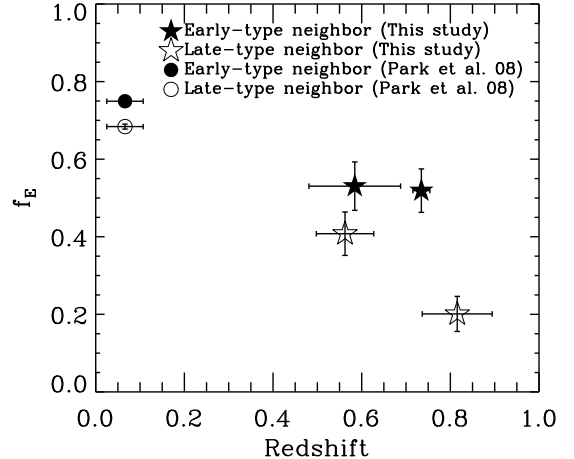


FIG. 9.— Dependence of the early-type fraction on the morphology of the nearest neighbor galaxy for the galaxies in the combined GOODS-North plus South sample. Filled and open star symbols indicate the early-type fraction for the early- and late-type neighbor cases in the GOODS-North plus South sample, respectively. The redshift bins are $0.4 \leq z \leq 0.7$ and $0.7 < z \leq 1.0$, and points are at the median redshifts. Circles denote the early-type fraction for the nearby galaxies in the SDSS (Park et al. 2008).

galaxies with $n > 2$ in the field does not change with redshift, while that in the high density region tends to increase toward the low redshift. When they use red galaxies with $u^* - g' > 1$, the fraction of red galaxies increases as redshift decreases in all environments. However, since they used photometric redshifts to estimate the local density, the environment was not accurately determined. In fact, Cooper et al. (2007) found no time evolution of the fraction of red galaxies in low density regions at $0.4 < z < 1.35$ using spectroscopic redshift data of DEEP2 galaxy redshift survey, though the number of red galaxies in their sample may be too small to draw a statistically significant conclusion.

Recently, Capak et al. (2007) used Gini parameter to select early-type galaxies in COSMOS data. They found that the early-type fraction in all environments grows as redshift decreases, and the growth rate is larger in high density regions compared to that in low density regions. However, in low density regions with < 100 galaxies Mpc^{-2} , the early-type fraction at $z > 0.4$ changes little with redshift. van der Wel et al. (2007) adopted a combination of Sérsic index n and bumpiness of galaxies as a proxy of galaxy morphology in SDSS and GOODS-South data. They found no time evolution of the early-type fraction at $z < 0.8$ for both cluster and field regions. They suggested that the reason why they could not find the evolution of the early-type fraction even in high density regions, is because they used mass-selected samples and different morphological classification from the other studies.

To confirm the environmental dependence of evolution of galaxy properties, we present the early-type fraction as a function of redshift in Figure 8. We divide our sample according to the redshift and the background density. It shows that the early-type fraction in high density regions is higher than that in low density regions in all redshift intervals explored. Moreover, the early-type fraction in high density regions increases much more rapidly as redshift decreases. It indicates a strong evolution of galaxy

morphology in high density regions, which is consistent with the observational results of some of previous studies and also with the predictions of Park et al. (2008).

Since our study indicates that the nearest neighbors derive the transformation of galaxy morphology, it is important to check galaxy morphology has evolved under strong influence of the nearest neighbors. Figure 9 is such an examination. We divided our sample into two subsets containing galaxies with early- or late-type neighbors. In this analysis we included only those galaxies that are interacting with neighbors ($r_p < r_{\text{vir,nei}}$). For the early-type fraction at low redshifts, we used the SDSS galaxies with $-20.0 > M_r > -21.5$ and $z < 0.1$ and whose magnitudes roughly fall into our M_B magnitude range (Choi et al. 2007; Park et al. 2008). Figure 9 clearly shows that the early-type fraction monotonically increases as redshift decreases, and the early-type fraction for the case of early-type neighbor is always larger than that for the late-type neighbor case. Primordial origin is not likely to be the reason for this systematic difference because the neighbor effects are limited within relatively tiny volume of the universe associated with each galaxy (see Fig. 5). As a comparison, the RMS displacement of matter in the flat Λ CDM universe is $7.7h^{-1}\text{Mpc}$ by $z=0.5$, more than an order magnitude larger than the virial radius of typical galaxies (Park & Kim 2009). This result demonstrates an important role of the nearest neighbor in the evolution of galaxy morphology, and is consistent with the prediction that the early-type fraction from high to low redshifts will increase because a series of interactions and mergers tend to transform late types into early types.

In summary, the early-type fraction in high density regions increases significantly as redshift decreases, while that in low density regions increases much more gently. The evolution of galaxy morphology is also found to depend critically on the small-scale environment, which is characterized by the morphology of the nearest neighbor galaxy and the distance to the nearest neighbor galaxy, in addition to the large-scale background density. A large sample of high redshift galaxies is needed to separate between the roles of small- and large-scale environments. We also found that isolated galaxies are brighter than less isolated ones. All these results are consistent with the predictions of Park et al. (2008), and confirm their unified scenario of transformation of galaxy morphology and luminosity class at high redshifts. It implies that galaxy-galaxy interactions play an important role in the evolution of morphology and luminosity classes of galaxies over a long period of time.

5. CONCLUSIONS

Using the spectroscopic sample of galaxies in the GOODS, we presented evidence for morphology and luminosity transformation of galaxies at $0.4 \leq z \leq 1.0$. We determined the morphological types of all high redshift galaxies by visual inspection, and used spectroscopic redshifts of galaxies to determine the environmental param-

eters. We examined the effects of the nearest neighbor galaxy and the local galaxy number density on the galaxy morphology. Our main results are as follows:

1. The early-type fraction increases with the surface galaxy number density estimated from 5th-nearest neighbor galaxies (Σ_5). This confirms the MDR followed by high redshift galaxies ($0.4 \leq z \leq 1.0$).
2. When a galaxy is located farther than the virial radius from its nearest neighbor galaxy, the probability for the galaxy to be an early type (f_E) decreases with increasing distance, and is independent of morphological type of the nearest neighbor.
3. When the separation with the nearest neighbor galaxy is smaller than the virial radius of the neighbor, f_E increases as the target galaxy approaches an early-type neighbor, but tends to stay constant as it approaches a late-type neighbor. Conformity in morphology between neighboring galaxies is confirmed at high redshifts. The realm of conformity is confined within the virialized region associated with each galaxy plus dark halo system.
4. We find that more isolated galaxies are more luminous. It can be explained by the luminosity evolution of galaxies through a series of mergers.
5. The early-type fraction f_E increases very rapidly as redshift decreases in high density regions, but increases only mildly in low density regions. At $z > 1$ the MDR seems very weak, and it should be confirmed by higher redshift data. Our findings are consistent with the prediction of Park et al. (2008) that the early-type fraction evolves much faster in high density regions than in low density regions because the rate of galaxy-galaxy interactions is higher in high density regions and a series of interactions and mergers through a cosmic time transform late types into early types.

The critical role of galaxy-galaxy interactions in the evolution of galaxy properties has been confirmed in the general environment (Park et al. 2008; Park & Choi 2009) and in the galaxy cluster environment (Park & Hwang 2008) at low redshifts. The results of the present work extend the previous findings to high redshifts. We plan to further extend our analysis to even higher redshift universe and to high redshift clusters.

We thank the anonymous referee for constructive comments that helped us to improve the manuscript. CBP acknowledges the support of the Korea Science and Engineering Foundation (KOSEF) through the Astrophysical Research Center for the Structure and Evolution of the Cosmos (ARCSEC).

REFERENCES

- Balogh, M. L., Baldry, I. K., Nichol, R., Miller, C., Bower, R., & Glazebrook, K. 2004a, *ApJ*, 615, L101
 Balogh, M., et al. 2004b, *MNRAS*, 348, 1355
 Blanton, M. R., Eisenstein, D., Hogg, D. W., Schlegel, D. J., & Brinkmann, J. 2005, *ApJ*, 629, 143
 Blanton, M. R., & Roweis, S. 2007, *AJ*, 133, 734
 Bundy, K., Ellis, R. S., & Conselice, C. J. 2005, *ApJ*, 625, 621

- Capak, P., Abraham, R. G., Ellis, R. S., Mobasher, B., Scoville, N., Sheth, K., & Koekemoer, A. 2007, *ApJS*, 172, 284
- Cassata, P., et al. 2007, *ApJS*, 172, 270
- Choi, Y.-Y., Park, C., & Vogeley, M. S. 2007, *ApJ*, 658, 884
- Cohen, J. G., Hogg, D. W., Blandford, R., Cowie, L. L., Hu, E., Songaila, A., Shopbell, P., & Richberg, K. 2000, *ApJ*, 538, 29
- Conselice, C. J., Blackburne, J. A., & Papovich, C. 2005, *ApJ*, 620, 564
- Conselice, C. J., Rajgor, S., & Myers, R. 2008, *MNRAS*, 386, 909
- Colless, M., et al. 2001, *MNRAS*, 328, 1039
- Cooper, M. C., et al. 2006, *MNRAS*, 370, 198
- Cooper, M. C., et al. 2007, *MNRAS*, 376, 1445
- Cooper, M. C., et al. 2008, *MNRAS*, 383, 1058
- Cowie, L. L., Barger, A. J., Hu, E. M., Capak, P., & Songaila, A. 2004, *AJ*, 127, 3137
- Cucciati, O., et al. 2006, *A&A*, 458, 39
- Davis, M., et al. 2007, *ApJ*, 660, L1
- Dressler, A. 1980, *ApJ*, 236, 351
- Dressler, A., et al. 1997, *ApJ*, 490, 577
- Elbaz, D., et al. 2007, *A&A*, 468, 33
- Faber, S. M., et al. 2007, *ApJ*, 665, 265
- Giavalisco, M., et al. 2004, *ApJ*, 600, L93
- Goto, T., Yamauchi, C., Fujita, Y., Okamura, S., Sekiguchi, M., Smail, I., Bernardi, M., & Gomez, P. L. 2003, *MNRAS*, 346, 601
- Hubble, E., & Humason, M. L. 1931, *ApJ*, 74, 43
- Lee, J. H., Lee, M. G., & Hwang, H. S. 2006, *ApJ*, 650, 148
- Le Fèvre, O., et al. 2004, *A&A*, 428, 1043
- Le Fèvre, O., et al. 2005, *A&A*, 439, 845
- Lotz, J. M., et al. 2008, *ApJ*, 672, 177
- Menanteau, F., et al. 2004, *ApJ*, 612, 202
- Mignoli, M., et al. 2005, *A&A*, 437, 883
- Nuijten, M. J. H. M., Simard, L., Gwyn, S., Röttgering, H. J. A. 2005, *ApJ*, 626, L77
- Oemler, A. J. 1974, *ApJ*, 194, 1
- Park, C., Choi, Y.-Y., Vogeley, M. S., Gott, J. R., & Blanton, M. R. 2007, *ApJ*, 658, 898
- Park, C., Gott, J. R., & Choi, Y.-Y. 2008, *ApJ*, 674, 784
- Park, C., & Choi, Y.-Y. 2009, *ApJ*, 691, 1828
- Park, C., & Hwang, H. S. 2008, *ApJ*, accepted (arXiv:0812.2088)
- Park, C., & Kim, Y.-R. 2009, *ApJ*, submitted (arXiv:0905.2268)
- Popesso, P., et al. 2009, *A&A*, 494, 443
- Poggianti, B. M., et al. 2008, *ApJ*, 684, 888
- Postman, M., & Geller, M. J. 1984, *ApJ*, 281, 95
- Postman, M., et al. 2005, *ApJ*, 623, 721
- Puzia, T. H., Mobasher, B., & Goudfrooij, P. 2007, *AJ*, 134, 1337
- Ravikumar, C. D., et al. 2007, *A&A*, 465, 1099
- Reddy, N. A., Steidel, C. C., Erb, D. K., Shapley, A. E., & Pettini, M. 2006, *ApJ*, 653, 1004
- Scoville, N., et al. 2007, *ApJS*, 172, 1
- Schlegel, D. J., Finkbeiner, D. P., & Davis, M. 1998, *ApJ*, 500, 525
- Smith, G. P., Treu, T., Ellis, R. S., Moran, S. M., & Dressler, A. 2005, *ApJ*, 620, 78
- Szokoly, G. P., et al. 2004, *ApJS*, 155, 271
- Tanaka, M., Goto, T., Okamura, S., Shimasaku, K., & Brinkmann, J. 2004, *AJ*, 128, 2677
- Treu, T., Ellis, R. S., Kneib, J.-P., Dressler, A., Smail, I., Czoske, O., Oemler, A., & Natarajan, P. 2003, *ApJ*, 591, 53
- van der Wel, A., et al. 2007, *ApJ*, 670, 206
- Vanzella, E., et al. 2005, *A&A*, 434, 53
- Vanzella, E., et al. 2006, *A&A*, 454, 423
- Vanzella, E., et al. 2008, *A&A*, 478, 83
- Weinmann, S. M., van den Bosch, F. C., Yang, X., & Mo, H. J. 2006, *MNRAS*, 366, 2
- Wirth, G. D., et al. 2004, *AJ*, 127, 3121
- York D. G. et al., 2000, *AJ*, 120, 1579